Cell

BLM Ortholog, Sgs1, Prevents Aberrant Crossing-over by Suppressing Formation of Multichromatid Joint Molecules

Steve D. Oh,[1] Jessica P. Lao,[1] Patty Yi-Hwa Hwang,[1] Andrew F. Taylor,[2] Gerald R. Smith,[2] and Neil Hunter[1,*]
[1] Sections of Microbiology and Molecular & Cellular Biology, University of California, Davis, One Shields Avenue, Davis, CA 95616, USA
[2] Division of Basic Sciences, Fred Hutchinson Cancer Research Center, 1100 Fairview Avenue North, P.O. Box 19024, Seattle, WA 98109, USA
*Correspondence: nhunter@ucdavis.edu
DOI 10.1016/j.cell.2007.05.035

SUMMARY

Bloom's helicase (BLM) is thought to prevent crossing-over during DNA double-strand-break repair (DSBR) by disassembling double-Holliday junctions (dHJs) or by preventing their formation. We show that the *Saccharomyces cerevisiae* BLM ortholog, Sgs1, prevents aberrant crossing-over during meiosis by suppressing formation of joint molecules (JMs) comprising three and four interconnected duplexes. Sgs1 and procrossover factors, Msh5 and Mlh3, are antagonistic since Sgs1 prevents dHJ formation in *msh5* cells and *sgs1* mutation alleviates crossover defects of both *msh5* and *mlh3* mutants. We propose that differential activity of Sgs1 and procrossover factors at the two DSB ends effects productive formation of dHJs and crossovers and prevents multichromatid JMs and counterproductive crossing-over. Strand invasion of different templates by both DSB ends may be a common feature of DSBR that increases repair efficiency but also the likelihood of associated crossing-over. Thus, by disrupting aberrant JMs, BLM-related helicases maximize repair efficiency while minimizing the risk of deleterious crossing-over.

INTRODUCTION

Homologous recombination (HR) occurs when a broken or damaged chromosome uses a homologous chromosome as template for its repair (Paques and Haber, 1999). HR can occur with one of two outcomes: a crossover, with exchange of chromosome arms, or a noncrossover involving only a local alteration of DNA. Unregulated crossing-over can cause chromosome rearrangements, missegregation, and homozygosis of deleterious mutations (Richardson et al., 2004). To minimize these risks, mitotically dividing cells actively suppress crossovers and preferentially utilize the sister chromatid as a repair template (Kadyk and Hartwell, 1992; Johnson and Jasin, 2001).

The RecQ family DNA helicase, Sgs1, acts to suppress mitotic crossing-over in budding yeast (Gangloff et al., 1994; Ira et al., 2003). Sgs1 is a homolog of human Bloom's helicase (BLM), which is mutated in the cancer-prone Bloom's Syndrome (Ellis et al., 1995; Watt et al., 1996). The signature of cells from Bloom's patients is unregulated crossing-over (Chaganti et al., 1974). In vitro studies show that RecQ proteins are bona fide DNA helicases with a preference for branched structures including joint molecule (JM) HR intermediates (Opresko et al., 2004). BLM disrupts D-loops, in which one DSB end has undergone strand-exchange with a homologous duplex, and both BLM and Sgs1 promote branch migration of Holliday junctions (HJs; Bennett et al., 1999; Karow et al., 2000; van Brabant et al., 2000; Bachrati and Hickson, 2006). Notably, combined action of BLM, its cognate type I topoisomerase TOPIIIα, and the specificity factor BLAP75/RMI1 can catalyze the "dissolution" of double-Holliday junctions (dHJs; Figure 2C) into two noncrossover duplexes (Wu et al., 2006; Wu and Hickson, 2003; Mullen et al., 2005; Plank et al., 2006). Hypercrossover phenotypes of both *sgs1* and *top3* mutants are consistent with the dissolvase model (Gangloff et al., 1994; Ira et al., 2003), but direct in vivo evidence for disruptase and/or dissolvase activities has been lacking.

During meiosis, HR plays essential roles in homolog pairing and segregation (Hunter, 2006; Petronczki et al., 2003). Most critically, crossing-over between homologs facilitates their stable bipolar connection to the meiosis I spindle and thereby promotes regular homolog disjunction. HR is an integral part of the meiotic program, being initiated by DNA double-strand breaks (DSBs) catalyzed by the transesterase Spo11 (Keeney, 2001). DSB ends are resected to form 3′-single-stranded tails that assemble into nucleoprotein filaments together with homologous-pairing and strand-exchange proteins, Rad51 and Dmc1 (Shinohara and Shinohara, 2004). The crossover or

noncrossover fate is thought to be determined at the next stage, as DSB ends pair with a homologous duplex and begin to exchange DNA strands (Allers and Lichten, 2001a; Bishop and Zickler, 2004; Borner et al., 2004; Hunter and Kleckner, 2001). Along the crossover pathway, two JM intermediates have been identified in vivo: single-end invasions (SEIs), which are thought to resemble D-loops (Hunter and Kleckner, 2001), and dHJs (see Figure 2C; Bell and Byers, 1983b; Schwacha and Kleckner, 1995; Allers and Lichten, 2001b; Cromie et al., 2006). dHJs are resolved to give crossover products (Allers and Lichten, 2001a; Hunter and Kleckner, 2001). Molecular events leading to noncrossovers are less clear but likely involve a synthesis-dependent strand-annealing (SDSA) mechanism. In its simplest form, SDSA proposes that one DSB end invades a homolog and primes DNA synthesis; the nascent strand is then displaced and anneals to complementary sequences on the second DSB end (Nassif et al., 1994; Paques and Haber, 1999).

At least eleven genes appear to specifically promote the crossover outcome of meiotic HR. These genes encode proteins of diverse molecular function: DNA helicase, Mer3; DNA exonuclease, Exo1; homologs of the MutS and MutL DNA mismatch-repair proteins, the Msh4-5 and Mlh1-3 heterocomplexes; a major component of synaptonemal complexes (SCs), Zip1; a SUMO E3 ligase, Zip3; large WD-like and TPR-like repeat proteins, Zip2 and Zip4; and a protein with no clear functional motifs, Spo16 (for review see Hunter, 2006; A. Shinohara, personal communication). All but three of these proteins are termed ZMMs (*Z*ip, *M*er, *M*sh) or SICs (*S*ynapsis *I*nitiation *C*omplex). ZMMs show meiosis-specific expression, and their mutation leads to coordinate defects in recombination and formation of SCs (e.g., Borner et al., 2004). The remaining three—Exo1, Mlh1, and Mlh3—function in mitotic and meiotic DNA mismatch correction, as well as meiotic crossing-over (Hoffmann and Borts, 2004; Kolas and Cohen, 2004). In contrast to *zmm* mutants, *exo1*, *mlh1*, and *mlh3* mutants form SCs normally. Moreover, *mlh1* and *mlh3* mutants appear to be defective at a later stage of HR than do *zmm* mutants (Lipkin et al., 2002; Woods et al., 1999) (N.H., A. Jambhekar, J.P.L., S.D.O., N. Kleckner and V.B. Borner, unpublished data).

In this study, we examine the function of Sgs1 in meiotic HR and its relationship to procrossover activities, represented by Msh5 and Mlh3. Our data argue that the major function of Sgs1 is not as a general regulator of the crossover/noncrossover decision; rather, Sgs1 acts at designated crossover sites, in conjunction with procrossover activities, to promote the orderly formation of interhomolog (IH) dHJs and productive crossing-over. In the absence of Sgs1, we detect high levels of a novel class of JMs that comprise three and four interconnected duplexes. Formation of these structures correlates with a specific increase in closely spaced double crossovers. We also provide direct in vivo evidence that Sgs1 suppresses dHJ formation between sister chromatids. These findings have broad implications for understanding meiosis, DSB repair, and the functions of BLM-related helicases.

RESULTS

Closely Spaced Double Crossovers Are Specifically Elevated in *sgs1-ΔC795* Mutants

To determine whether mutation of *SGS1* causes a general increase in crossing-over, we utilized a diploid strain in which crossing-over within nine different intervals, located on three different chromosomes, can be scored in a single cross (Figure 1A; Experimental Procedures). We also utilized the *sgs1-ΔC795* truncation mutation (Mullen et al., 2000) because, as shown by Rockmill et al. (2003), cells carrying this mutation sporulate more efficiently than *sgs1Δ* null mutants, and their vegetative growth rate is essentially normal. Sgs1-ΔC795 protein lacks the conserved helicase, RQC, and HRDC domains but retains the N-terminal region implicated in several protein-protein interactions (Bachrati and Hickson, 2003). Wild-type and *sgs1-ΔC795* cells were sporulated and segregation patterns analyzed by tetrad analysis (Figure 1; Supplemental Data, Figure S1 and Tables S1–S4). At least one interval along each of the three chromosomes analyzed shows a significant increase in map distance (Figure 1C and Tables S1 and S2). The largest increase, almost 1.7-fold, is observed along chromosome 3 in the interval *LEU2-CEN3*. Overall, however, the combined map distance for all intervals is increased by a modest 1.17-fold (from 165 cM in wild-type to 193 cM in *sgs1-ΔC795*).

In a single genetic interval, various crossover classes are detected by tetrad analysis (Figure 1B): double crossovers involving all four chromatids result in a nonparental ditype tetrad (NPD); single crossovers or double crossovers involving three chromatids produce tetratype tetrads (TT); and zero crossovers or double crossovers involving the same two chromatids produce parental ditype tetrads (PD). Close inspection of *sgs1-ΔC795* tetrad data reveals that expanded map distances are attributable to a disproportionate increase in closely spaced double crossovers, as represented by NPD tetrads (Figure 1C and Table S1). This pattern is not expected from a general increase in crossing-over, i.e., all DSBs having an increased probability of a crossover outcome, which predicts a decrease in the zero (PD) tetrad class and proportional increases in single (TT) and double (NPD) crossover tetrads. The unique alteration of crossing-over in *sgs1-ΔC795* cells is further illustrated by comparing distributions of crossover classes for the combined intervals along each of the three analyzed chromosomes (Figure 1D). For each chromosome, the fraction of *sgs1-ΔC795* tetrads with zero detectable crossovers remains unchanged or is increased, the fraction with one detectable crossover is decreased, and the fractions with two and three or more crossovers are increased.

Adjacent crossovers between the same pair of homologs tend to be widely and evenly spaced, a phenomenon known as positive crossover interference (Muller, 1916). The disproportionate increase in double crossovers in

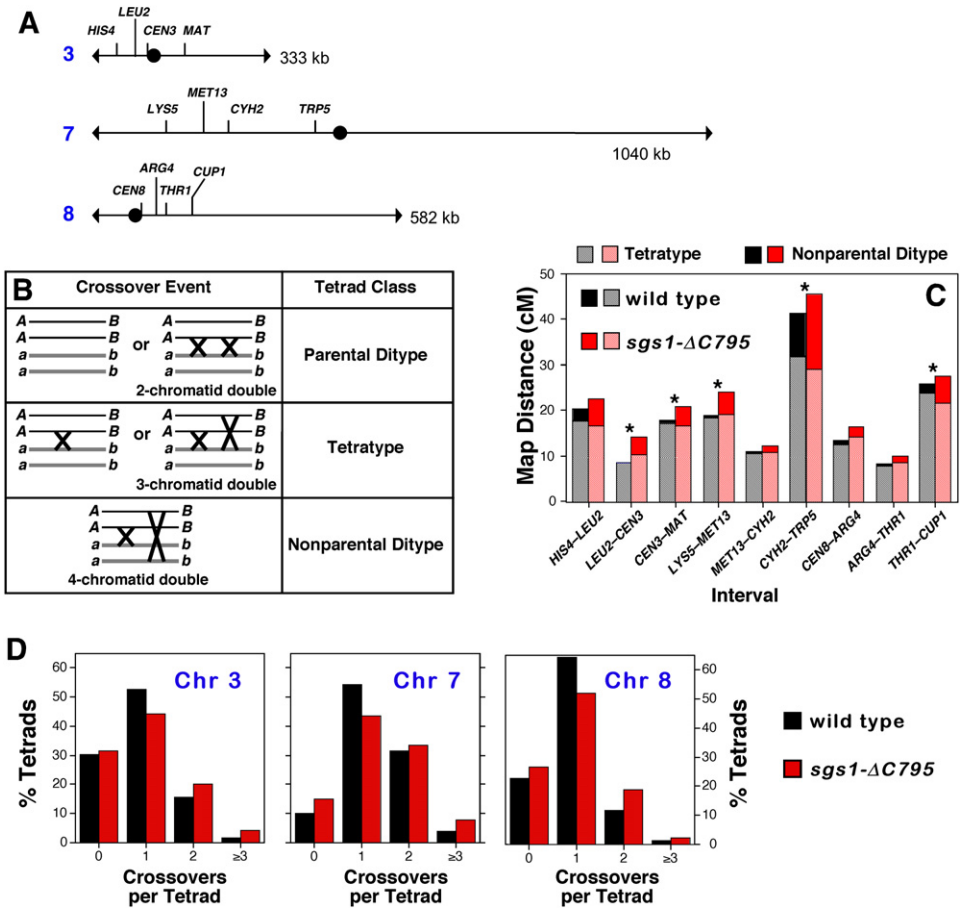

Figure 1. Tetrad Analysis of Wild-Type and *sgs1-ΔC795* Cells

(A) Intervals analyzed. CEN3 is marked with the *ADE2* gene; CEN8 is marked with *URA3*.

(B) Crossover classes within a single interval and their genetic outcomes.

(C) Contributions of tetratype and non-parental ditype tetrads to map distances in wild-type and *sgs1-ΔC795* strains. Asterisks indicate significant differences between map distances in wild-type and *sgs1-ΔC795* tetrads (see Tables S1 and S2; spore viability data are shown in Figure S1).

(D) Distribution of crossover classes for the combined intervals along the three chromosomes analyzed. Wild-type and *sgs1-ΔC795* distributions differ significantly for each chromosome: chromosome 3, $p = 0.0008$; chromosome 7, $p = 3 \times 10^{-5}$; chromosome 8, $p = 1 \times 10^{-5}$.

sgs1-ΔC795 cells suggests that positive crossover interference may be diminished. This inference is confirmed by additional analysis presented in Figure S2 and Tables S3 and S4.

Taken together, tetrad analysis indicates that while the *sgs1-ΔC795* mutation moderately increases map distances, its major effect is not a general increase in the probability that any initiated recombination event will become a crossover. Rather, it appears that a fraction of the events that would normally form single crossovers in wild-type cells gives rise to closely spaced double crossovers in *sgs1-ΔC795* cells.

Intersister-dHJs Are Elevated in *sgs1-ΔC795* Cells

To understand the molecular defects underlying the aberrant crossover patterns in *sgs1-ΔC795* cells, we analyzed the DNA events of recombination using the *HIS4LEU2* physical assay system (Figure 2; Schwacha and Kleckner, 1995; Hunter and Kleckner, 2001). DNA events are monitored over time in synchronized cultures induced to undergo meiosis. Cell samples are treated with psoralen to produce DNA interstrand crosslinks, which stabilize SEI and dHJ intermediates. Species of interest are detected by gel electrophoresis and Southern hybridization with Probe 4 (Figure 2). XhoI polymorphisms between parental "Mom" and "Dad" homologs produce diagnostic restriction fragments for parental and recombinant chromosomes, DSBs, and JMs (SEIs and dHJs). In addition, Mom and Dad chromosomes can be distinguished by probing for short heterologous insertions of ØX174 DNA ("Probe Mom" and "Probe Dad" in Figure 2A; Schwacha and Kleckner, 1994). Each hybridizing signal is quantified using a Phosphorimager. DSBs and crossovers are quantified from one-dimensional gels (Figure 2B). Native/native two-dimensional gels reveal the branched structure of JMs and are used to quantitate SEIs and dHJs (Figures

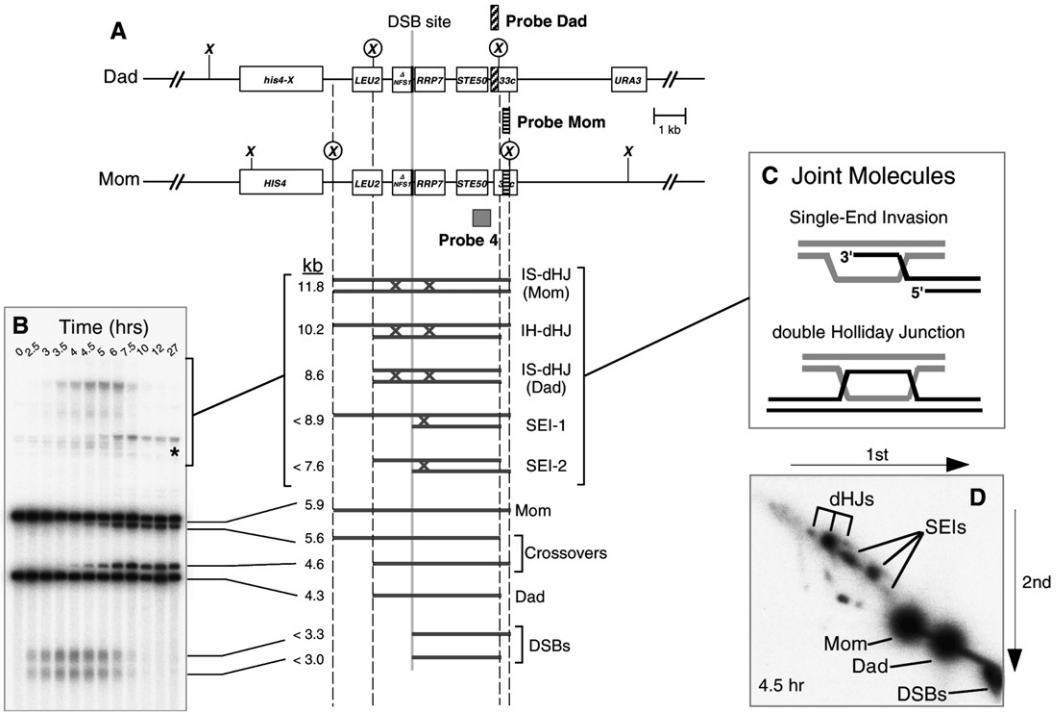

Figure 2. Physical Assay System for Monitoring Recombination

(A) Map of the *HIS4LEU2* locus showing diagnostic restriction sites and the positions of probes. DNA species detected with Probe 4 are shown below. SEI-1 and SEI-2 are the two major SEI species detected with Probe 4 (see Hunter and Kleckner, 2001).

(B) Image of one-dimensional (1D) gel hybridized with Probe 4 showing DNA species detailed in (A). Asterisk indicates a meiosis-specific recombinant band resulting from "gene conversion" of the most DSB-proximal XhoI site.

(C) Presumed structures of SEI and dHJ joint molecules.

(D) Image of native/native two-dimensional (2D) gel hybridized with Probe 4. Species detailed in (A) are highlighted. The three dHJ species are highlighted by a trident; SEIs are indicated by a fork.

2C and 2D; Bell and Byers, 1983a; Hunter and Kleckner, 2001). To monitor the timing and efficiency of meiotic divisions, fixed cells are stained with DAPI and scored as having one, two, or four nuclei.

Wild-type and *sgs1-ΔC795* cultures were sporulated and analyzed in parallel. Analysis of one pair of time courses is described below and in Figure 3. Data for two additional pairs of time courses are presented in Figure S3. Although the absolute levels of recombination intermediates vary between time courses, all paired experiments are internally consistent and identical conclusions can be drawn.

DSBs

In wild-type cells, DSBs are detected 2.5 hr after induction of meiosis, peak at 4.5 hr, and are gone by 7 hr (Figure 3A). The timing and level of DSBs in *sgs1-ΔC795* cells are very similar to wild-type except that a small number of DSBs may turn over more slowly.

Crossovers and Meiotic Divisions

Crossover bands first appear at 4 hr for wild-type meiosis and plateau after 8 hr at 19.7% of hybridizing DNA. In *sgs1-ΔC795* cells, crossovers show a very slight delay (≤30 min) and plateau at 18.1% of hybridizing DNA. This slight reduction in crossover frequency contradicts tetrad data, which show that crossing-over at *HIS4LEU2* is, in fact, slightly increased in *sgs1-ΔC795* cells (29.9 cM versus 26.9 cM in wild-type; see Tables S5 and S6). A possible explanation is that a small fraction of *sgs1-ΔC795* cells fail to enter meiosis or to complete the first meiotic division, as reflected by the reduced efficiency of meiotic divisions in this strain (88% versus 97% in wild-type; Figure 3A). Correcting for this difference gives a maximum crossover level of 19.9% for the *sgs1-ΔC795* time course shown in Figure 3. By averaging measurements from three independent time courses for both wild-type and *sgs1-ΔC795* strains, a more accurate comparison of crossing-over was made. An average of 19.0% ± 0.6% (SE) crossovers was recorded for the three wild-type experiments compared to 19.9% ± 1.5% for *sgs1-ΔC795* time courses. In each case, meiotic divisions in *sgs1-ΔC795* time courses were less efficient (88%, 85%, and 88% versus 94%, 95%, and 97%). Assuming this difference reflects cells that failed to undergo meiosis, crossing-over could be as high as 21.7% ± 1.5% in *sgs1-ΔC795* cells. This ~1.14-fold increase is consonant with the ~1.11-fold increase measured by tetrad analysis (above). In summary, crossing-over at *HIS4LEU2* is either unaffected or slightly increased by the *sgs1-ΔC795* mutation.

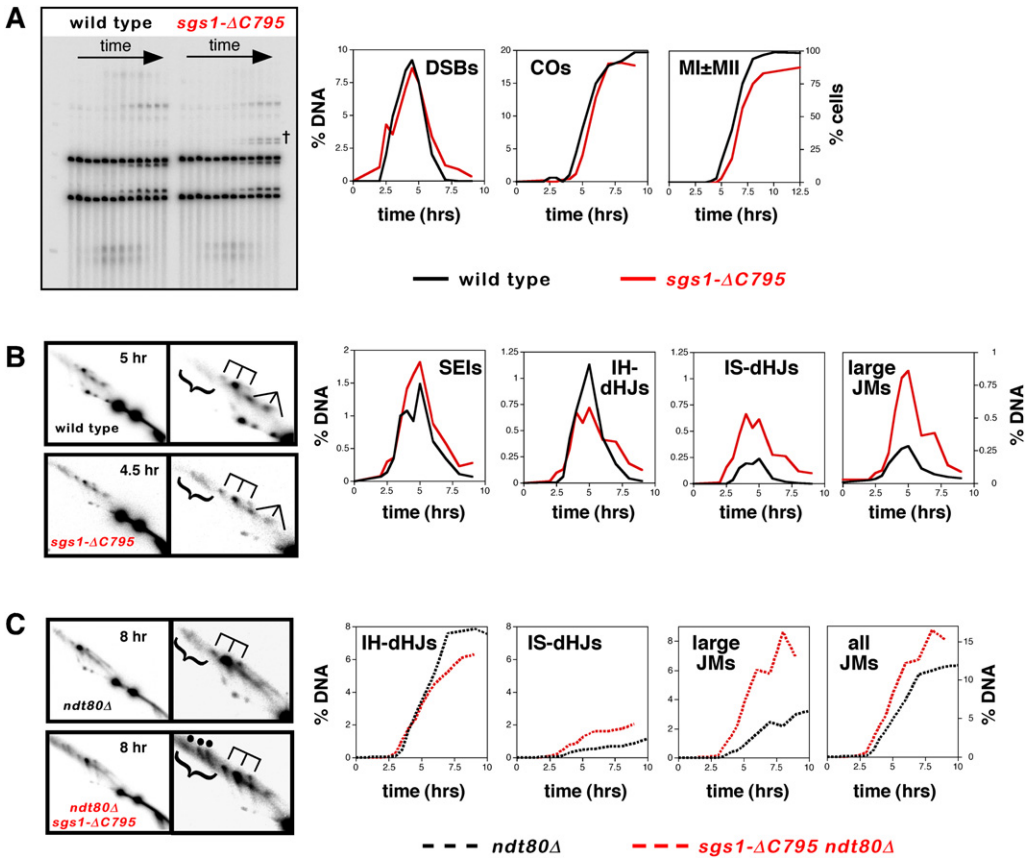

Figure 3. Physical Analysis of Recombination in Wild-Type and *sgs1-ΔC795* Cells

(A) 1D analysis of DSBs and crossovers (COs), and analysis of meiotic divisions (MI ± MII). % DNA is percent of total hybridizing DNA. MI ± MII is cells that have completed either the first or second meiotic divisions. †, bands resulting from ectopic recombination between *HIS4LEU2* and the *leu2::hisG* allele at the native *LEU2* locus (see Grushcow et al., 1999). The role of Sgs1 in preventing these events will be described elsewhere (unpublished data).

(B) 2D analysis of joint molecules in *NDT80* cells. In each case a representative 2D panel is shown together with a blowup of the JM region. dHJ species are highlighted by a trident; SEIs are indicated by a fork; large JMs are bracketed.

(C) 2D analysis of joint molecules in *ndt80Δ* cells. "all JMs" = IH-dHJs + IS-dHJs + large JMs.

See also Figure S2.

SEIs

In both wild-type and *sgs1-ΔC795* cells, SEIs form with similar kinetics and peak at ~5 hr (Figure 3B). SEIs reach slightly higher levels over several time points in *sgs1-ΔC795* cells, but this difference does not appear to be reproducible (Figure S2).

dHJs

Restriction site polymorphisms between Mom and Dad homologs allow interhomolog dHJs (IH-dHJs) to be distinguished from intersister dHJs (IS-dHJs) (Figures 2A and 2D; Schwacha and Kleckner, 1997). In wild-type cells, IH-dHJs form with a ~4.7-fold bias over IS-dHJs (peak steady-state levels of 1.13% for IH-dHJs versus 0.24% for IS-dHJs; Figure 3B). This strong interhomolog bias is diminished in *sgs1-ΔC795* mutant cells. Peak steady-state levels of IH-dHJs are slightly reduced relative to wild-type (0.72% versus 1.13%), whereas IS-dHJs are increased ~2.5-fold (0.61% versus 0.24%).

ndt80Δ Analysis

The apparent reduction of IH-dHJs in *sgs1-ΔC795* cells is surprising, especially given that crossovers reach at least wild-type levels. To rule out the possibility that a subset of IH-dHJs turn over faster in *sgs1-ΔC795* cells, we measured dHJ levels in an *ndt80Δ* background, which causes cells to arrest in pachytene and accumulate dHJs (Figure 3C; Allers and Lichten, 2001a). This analysis confirms the inferences made in *NDT80* cells. Specifically, IH-dHJs accumulate to ~25% lower levels in *sgs1-ΔC795* cells (7.9% in wild-type versus 6.3% in *sgs1-ΔC795*), and IS-dHJs reach ~2-fold higher levels (0.87% in wild-type versus 1.75% in *sgs1-ΔC795*). Joint molecule analysis from *ndt80Δ* cells differs from that in *NDT80* cells in that interhomolog bias appears to be more extreme in the *ndt80Δ* data set (4.7-fold versus 9-fold for *SGS1* cells, and 1.2-fold versus 3.6-fold in *sgs1-ΔC795* mutants). The reason for this difference is unclear. IH-dHJs and

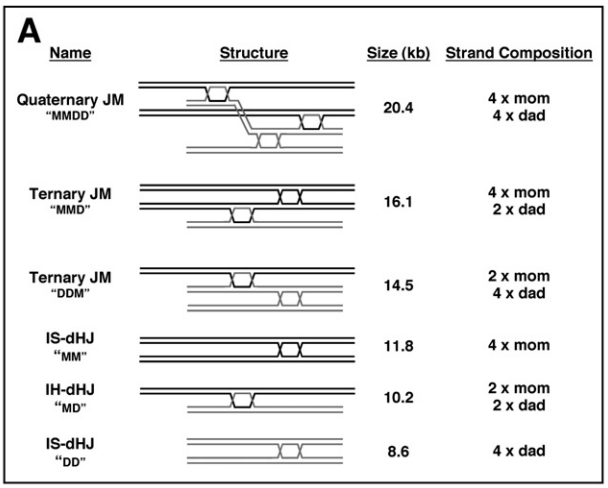

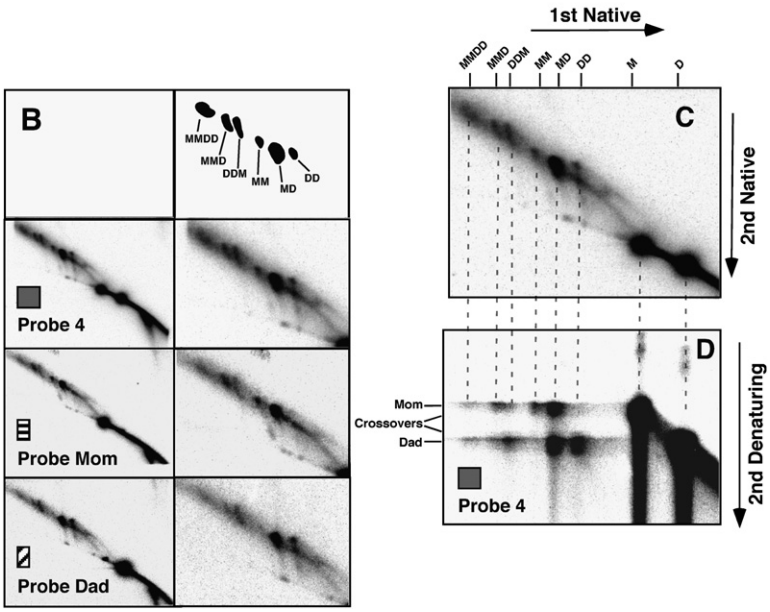

Figure 4. Large JMs Contain Three and Four Chromatids

(A) Predicted structures, sizes, and DNA strand composition of joint molecule species.

(B) Sequential probing of an 8 hr sample from an *sgs1-ΔC795 ndt80Δ* time course with common probe, Probe 4, and homolog-specific probes, Probe Dad and Probe Mom (see Figure 2). Full panels from native/native 2D gels are shown on the left and blowups are shown on the right. Interpretative cartoon shows the positions of the JM species detailed in (A).

(C and D) "Pull-apart" analysis of component strands of the large JMs. (C) Native/native 2D gel highlighting the species of interest. (D) Native/denaturing 2D gel showing that large JMs comprise parental-length component single strands.

IS-dHJs may have different life spans in *NDT80* cells, or *ndt80Δ* may differentially affect the resolution of IH-dHJs relative to IS-dHJs. Regardless, this difference does not alter the basic inference that the *sgs1-ΔC795* mutation decreases IH-dHJs and increases IS-dHJs.

Novel High-Molecular-Weight JMs Form at High Levels in *sgs1-ΔC795* Cells

sgs1-ΔC795 ndt80Δ analysis reveals three prominent, high-molecular-weight JM species on two-dimensional (2D) gels (bracketed signals in Figure 3C; individual species highlighted by dots; also see Figures 4B and 4C). Two of these appear as discrete signals with sizes in the ~14–17 kb range and their relative levels are essentially equal; a third signal is less discrete and larger, at ~20 kb. These species can also be detected in wild-type, *sgs1-ΔC795*, and *ndt80Δ* strains (Figures 3B and 3C) but the *sgs1-ΔC795* mutation significantly increases their levels, by ~3-fold in both *NDT80* and *ndt80Δ* backgrounds. Thus, large JMs are a major recombination intermediate during meiosis in *sgs1-ΔC795* cells. Overall, when IH-dHJ, IS-dHJ, and large JM signals are added together, *sgs1-ΔC795* cells form ~35% more JMs than wild-type cells due to conspicuous increases in IS-dHJs and large JMs.

Large JMs Comprise Three or Four Interconnected Homologous Chromatids

The prominence of large JMs in *sgs1-ΔC795* meiosis makes it critical to ascertain their identity. An attractive possibility is that large JMs comprise more than two duplexes, interconnected by HJs (Figure 4A). Predicted sizes of these ternary and quaternary JMs are consistent with sizes of the large JMs detected on 2D gels: two Dad chromatids plus one Mom chromatid will produce a JM of 14.5 kb (ternary JM "DDM"); two Moms plus one Dad will give a JM of 16.1 kb (ternary JM "MMD"); and two

Moms plus two Dads will form a JM of 20.4 kb (quaternary JM "DDMM"). Notably, the latter species can be resolved to give two closely spaced interhomolog crossovers (see Figure 7C).

To confirm the identity of large JMs, their composition was analyzed in two ways. First, 2D gels were hybridized with probes specific to either Mom or Dad homologs (Figures 2A and 4B). With "Probe Mom," the predicted pattern is observed; the larger of the two parental linear bands (1 × Mom), the IH-dHJ spot (Mom + Dad), and the larger of the two IS-dHJ spots (2 × Mom) are detected. In addition, Probe Mom detects the three large JM species; notably, the middle size species produces a signal with twice the intensity of the smaller species (signal ratio of 1.9:1.0), consistent with the prediction that the two ternary JMs should contain different numbers of Mom and Dad chromatids. With "Probe Dad" the reciprocal pattern is detected: the smaller parental linear band (1 × Dad), the IH-dHJ (Mom + Dad), the smaller IS-dHJ (2 × Dad), plus the three large JMs. Moreover, the relative intensity of the middle and smaller species is the reverse of that seen with Probe Mom (ratio of 1.0:1.9). Relative signal intensities for the largest JM (1.2:1.0) indicate approximately equal numbers of Mom and Dad chromatids, as expected for a quaternary JM.

We also analyzed component strands of large JMs using native/denaturing 2D gels in which psoralen crosslinks are removed prior to running the second dimension under denaturing conditions (Figure 4D). If large JMs contain three or four homologous duplexes interconnected by either dHJs or hemicatenanes, the component strands should all be parental in length, i.e., Mom- and Dad-length strands (Figure 4A). In the second dimension, as shown previously, IH-dHJs are denatured into Mom- and Dad-length strands, and the two IS-dHJs comprise either Mom or Dad strands (Schwacha and Kleckner, 1995). As predicted, large JMs are denatured into primarily parental-length Mom and Dad strands, consistent with proposed structures of three and four duplexes interconnected by two or three dHJs. Recombinant-length strands are not prominent, indicating that large JMs do not generally include single HJs (or odd numbers of HJs). Thus, large JMs most likely comprise three and four chromatids interconnected by dHJs. We cannot rule out the possibility that a fraction of multichromatid JMs are connected by one or more single HJs, however.

Comparing relative levels of parental-length single strands in ternary and quaternary JMs confirms the inferences made using homolog-specific probes (above). The quaternary JMs comprise approximately equal levels of Mom and Dad strands (~1.0:1.0), while the two ternary JMs, MMD and DDM, contain, respectively, ~1.7:1.0 and ~1.0:1.9 ratios of Mom:Dad strands (see Experimental Procedures).

Direct Visualization of Multichromatid JMs by Electron Microscopy

The molecular analysis above is consistent with the idea that large JMs are intermediates containing three and four homologous duplexes. To visualize these structures directly, branched molecules from genomic DNA of *ndt80Δ SGS1* and *ndt80Δ sgs1-ΔC795* cells were purified from 2D gels and examined by electron microscopy (EM) (Figure 5; Bell and Byers, 1983b; Cromie et al., 2006). Note that, unlike analysis at *HIS4LEU2,* this method visualizes JMs formed at loci throughout the genome.

Random sampling of EM grids reveals significantly different distributions of molecule types in *ndt80Δ*

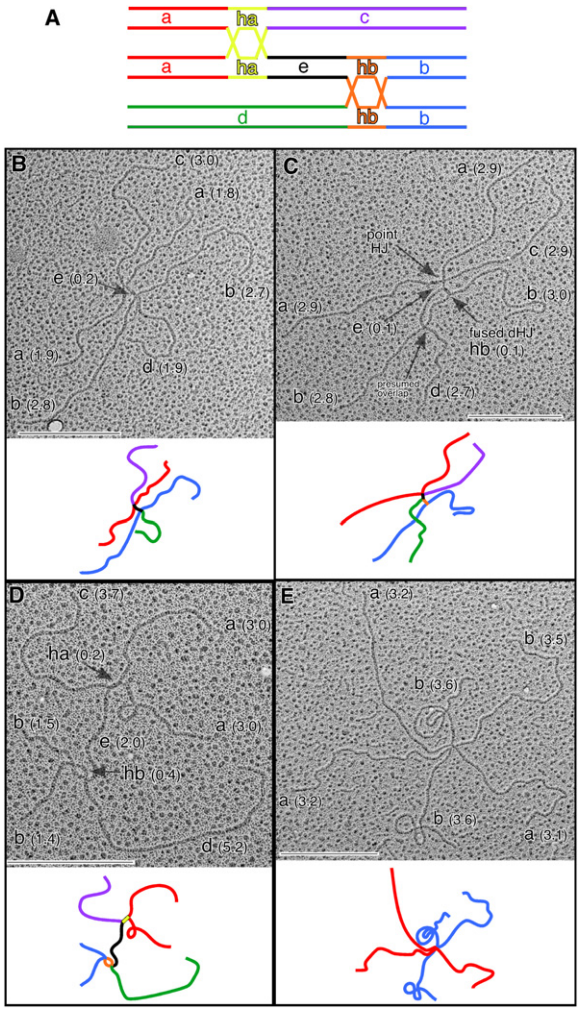

Figure 5. Direct Visualization of Ternary JMs by Electron Microscopy

(A) Predicted relationships between segment lengths for fully homologous ternary JMs. (B–E) EM images and interpretative cartoons of ternary JMs from an *sgs1-ΔC795 ndt80Δ* DNA sample taken at 8 hr: (B) ternary JM comprising three ~4.8 kb molecules interconnected by two closely spaced point junctions; (C) three ~4.8 kb molecules connected by a fused dHJ structure and a point junction; (D) three ~6.9 kb molecules connected by an open dHJ and a fused dHJ; (E) three 6.7 kb molecules connected at a single point, presumably by two very closely spaced point junctions. Segments correspond to those shown in (A). Lengths are in kb (see Experimental Procedures). Scale bars = 0.5 μm. See also Figures S3 and S4.

SGS1 and *ndt80Δ sgs1-ΔC795* samples. Six classes of molecules can be discerned by EM (Figures 5, S4, and S5 and data not shown): linear molecules; Y-structures; binary JMs with four free ends (canonical HJs; e.g., Figure S5F); ternary JMs with six ends; quaternary JMs with eight ends; and complex JMs with more than eight ends. JMs are interconnected by combinations of open dHJs, fused dHJs, and point junctions, which could be single HJs or two very closely spaced HJs. In the *ndt80Δ SGS1* sample, we counted 42 linears, 8 Ys, 55 binary JMs, 2 ternary JMs, 1 quaternary JM, and no JMs with >8 ends. Consistent with the analysis at *HIS4LEU2*, multichromatid JMs are significantly enriched in the *ndt80Δ sgs1-ΔC795* sample, in which we counted 42 linears, 5 Ys, 58 binary JMs, 13 ternary JMs, 4 quaternary JMs, and 3 JMs with >8 ends, representing a 5.8-fold increase in ternary and quaternary JMs ($p = 0.012$ by *G*-test).

Ternary JMs are predicted to have six arms with the length relationships shown in Figure 5A. Ten of twenty-one six-armed structures analyzed showed exactly this relationship and can confidently be assigned as ternary JMs (Figures 5 and S4). In the other 11 six-armed JMs, one or more predicted arm lengths differed from expectations by >15%. Such structures have a variety of possible explanations, e.g., illegitimate strand-exchange (homeologous or nonhomologous), strand-exchange within repetitive sequences (tandem or dispersed), hemicatenane formation at one or more junction points, and partial digestion or damage to the DNA during sample preparation. We can conclude, however, that ternary JMs of the predicted structure are a regular feature of *sgs1-ΔC795* meiosis. While the largest JMs formed at *HIS4LEU2* clearly have the size, mobility, and strand composition expected for quaternary JMs (Figure 4), we have been unable to unambiguously assign this structure to eight-armed molecules observed by EM (Figure S5). Nonetheless, EM analysis clearly confirms the inferences made by analysis of DNA events at *HIS4LEU2*, i.e., that Sgs1 inhibits the formation of aberrant multichromatid JMs or promotes their disassembly.

sgs1-ΔC795 Relieves the Crossover Defects of *mlh3Δ* and *msh5Δ* Mutants

Two-hybrid and immunoprecipitation assays have demonstrated an interaction between Sgs1 or BLM and the Mlh1-Mlh3 complex (Langland et al., 2001; Pedrazzi et al., 2001; Wang and Kung, 2002), but the biological relevance of this interaction is unclear. Also, Sgs1 immunostaining foci show extensive colocalization with pro-crossover factors along pachytene SCs (Rockmill et al., 2003). Similarly, in mouse, BLM colocalizes with the MutS homolog MSH4 (Moens et al., 2002). To understand the relationship between the specialized anticrossover function of Sgs1, identified here, and meiotic procrossover functions, we examined the interaction between the *sgs1-ΔC795* allele and deletion mutations of the *MLH3* and *MSH5* genes (Msh5 acts in a complex with Msh4; Pochart et al. [1997]). An isogenic set of single- and double-mutant strains was constructed and crossing-over was analyzed by tetrad analysis.

Crossing-over in the two intervals flanking *HIS4LEU2* is reduced by ~1.4-fold in *mlh3Δ* mutants and ~1.7-fold in *msh5Δ* mutants, consistent with published data (Figures 6A and 6B and Tables S5 and S6; Argueso et al., 2004; Hollingsworth et al., 1995; Wang et al., 1999). Strikingly, introduction of the *sgs1-ΔC795* allele into *mlh3Δ* and *msh5Δ* mutant backgrounds completely restores crossing-over to at least wild-type levels. In fact, in *msh5Δ sgs1-ΔC795* tetrads, map distances are significantly larger than in wild-type, more closely resembling the *sgs1-ΔC795* single mutant (Tables S5 and S6). Importantly, however, the small increases in map distance observed in *sgs1-ΔC795* tetrads (<1.2-fold) cannot account for the large increases seen in *mlh3Δ sgs1-ΔC795* (1.6- to 1.8-fold) and *msh5Δ sgs1-ΔC795* (2.0- to 2.5-fold) double mutants. We infer that Sgs1 is responsible for the crossover defects of *mlh3Δ* and *msh5Δ* mutants.

Reduced crossing-over in *msh5Δ* and *mlh3Δ* mutants causes homologs to missegregate, which in turn results in some dead spores (Figure 5B; Argueso et al., 2004; Hollingsworth et al., 1995). Suppression of *mlh3Δ* and *msh5Δ* crossover defects by *sgs1-ΔC795* is therefore expected to improve spore viability. This is clearly the case for *msh5Δ sgs1-ΔC795* cells, which produce 82% viable spores compared to 44% for the *msh5Δ* single mutant (Figure 6B). While this is still lower than the 96% viable spores observed for wild-type, *msh5Δ sgs1-ΔC795* spore viability is not significantly different from that of the *sgs1-ΔC795* single mutant (78%). The situation is less obvious for the *mlh3Δ* and *mlh3Δ sgs1-ΔC795* comparison, which produce 81% and 78% viable spores, respectively. However, the effects of the two mutations on spore viability are clearly not additive (expected viability, 63%). In fact spore viability of the *mlh3Δ sgs1-ΔC795* strain is also indistinguishable from that of the *sgs1-ΔC795* single mutant. We conclude that *sgs1-ΔC795* relieves both crossover and homolog segregation defects of *msh5Δ* and *mlh3Δ* mutants.

This analysis indicates that Sgs1 can function as a general anticrossover factor when procrossover activities, such as Msh5 or Mlh3, are absent. *sgs1* mutation has recently been shown to variably suppress the crossover defects of *zmm* mutants, *msh4Δ, mer3Δ, zip1Δ*, and *zip2Δ* (Jessop et al., 2006). Together, these data imply that procrossover activities of ZMMs generally antagonize Sgs1 during meiosis (but see Discussion).

The dHJ Formation Defect of *msh5Δ* Cells Is Relieved by the *sgs1-ΔC795* Mutation

Sgs1 could prevent crossing-over by disrupting primary strand-exchange products, such as SEIs, and/or by dissolving dHJs in a concerted reaction together with the type I topoisomerase Top3 (see Introduction). To test these ideas, we analyzed intermediate steps of HR in *msh5Δ* and *msh5Δ sgs1-ΔC795* cells by physical analysis at *HIS4LEU2* (Figures 6C, 6D, and 6E).

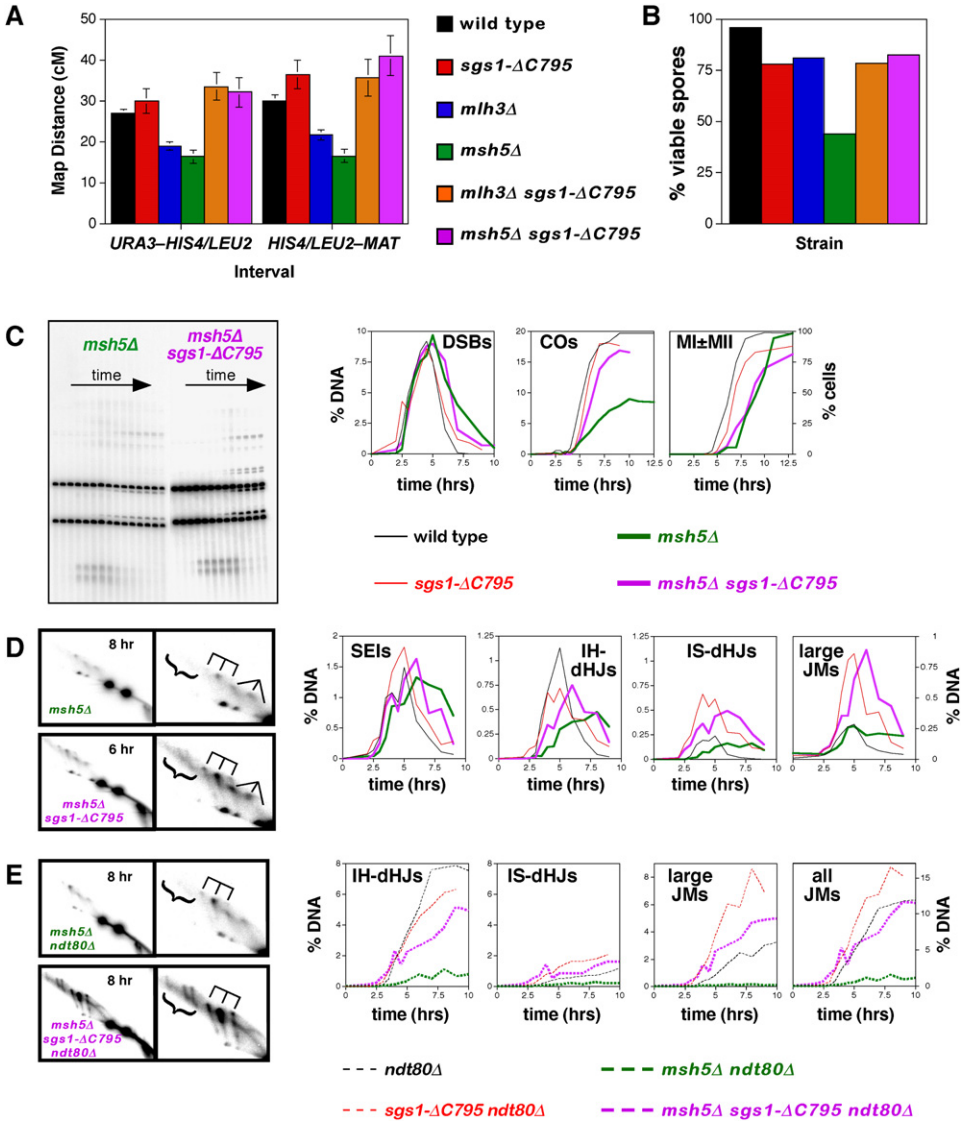

Figure 6. *sgs1-ΔC795* Relieves the Crossover Defects of *msh5Δ* and *mlh3Δ* Mutants

(A) Tetrad analysis of crossing-over in two intervals flanking the *HIS4LEU2* locus. Error bars indicate standard errors. See Tables S5 and S6.

(B) Spore viability. At least 200 tetrads were dissected for each strain.

(C) 1D analysis of DSBs and crossovers (COs) and analysis of meiotic divisions (MI ± MII) from *msh5Δ* and *msh5Δ sgs1-ΔC795* time course experiments. Data for wild-type and *sgs1-ΔC795* cells are from Figure 3A.

(D) 2D analysis of joint molecules in *msh5Δ* and *msh5Δ sgs1-ΔC795*.

(E) 2D analysis of joint molecules in *msh5Δ ndt80Δ* and *msh5Δ sgs1-ΔC795 ndt80Δ* cells.

DSBs

In *msh5Δ* cells, DSBs form normally, but their turnover is significantly delayed, consistent with previous analysis (Figure 6C; Borner et al., 2004). By 10 hr, however, DSBs have disappeared, indicating efficient repair. In *msh5Δ sgs1-ΔC795* cells, turnover is still delayed relative to wild-type and *sgs1-ΔC795* cells, but DSBs disappear faster than in the *msh5Δ* single mutant.

Crossovers and Meiotic Divisions

Suppression of *msh5Δ* and *mlh3Δ* crossover defects by *sgs1-ΔC795* is confirmed by physical assays (Figure 6C; for analysis of *mlh3Δ*, see Figure S6). Crossing-over in *msh5Δ* cells is reduced 2.2-fold, relative to wild-type. In the *msh5Δ sgs1-ΔC795* double mutant, crossing-over is restored to near wild-type levels, reaching 17.1% of hybridizing DNA compared to 19.7% in wild-type cells. Correcting for the fact that *msh5Δ sgs1-ΔC795* strains undergo meiosis slightly less efficiently than wild-type (Figure 6C) gives a crossover level of 20.2%, which implies complete restoration of crossing-over, consistent with tetrad analysis. Notably, however, *msh5Δ sgs1-ΔC795* strains retain characteristics of the *msh5Δ* single mutant,

specifically slight delays in DSB turnover, crossover formation, and meiotic divisions (Figure 6C).

SEIs

msh5Δ strains form SEIs more slowly than wild-type (Figure 6D; Borner et al., 2004). High steady-state levels of SEIs do eventually form but then persist until very late times, suggesting an additional defect at the SEI-to-dHJ transition. In *msh5Δ sgs1-ΔC795* cells, these phenotypes are at least partially suppressed, with faster formation and turnover of SEIs. Clearly, however, the kinetics of SEI formation are still somewhat aberrant in *msh5Δ sgs1-ΔC795* relative to wild-type and *sgs1-ΔC795* strains.

dHJs

In *msh5Δ* cells, IH-dHJ levels peak ~3 hr later than in wild-type and *sgs1-ΔC795* cells and reach lower levels (0.47%, 1.17%, and 0.72%, respectively). Again, *sgs1-ΔC795* partially suppresses the *msh5Δ* phenotype: IH-dHJs form with a delay of only ~1 hr and peak at the same level as in the *sgs1-ΔC795* single mutant. Formation of IS-dHJs in *msh5Δ* and *msh5Δ sgs1-ΔC795* cells follows similar patterns as those described for IH-dHJs. In this case, however, the *msh5Δ sgs1-ΔC795* double mutant more clearly resembles the *sgs1-ΔC795* single mutant, forming higher than normal levels of IS-dHJs.

Large JMs

Large JMs can be detected in *msh5Δ* cells. They form with relatively normal kinetics and reach near-wild-type levels but then persist at late times (Figure 6D). In the *msh5Δ sgs1-ΔC795* double mutant, this pattern changes dramatically. Similar to the situation seen in the *sgs1-ΔC795* single mutant, high levels of large JMs are seen in *msh5Δ sgs1-ΔC795* cells, although their appearance is delayed by ~1 hr.

ndt80Δ Analysis

Analysis of accumulated JMs in *ndt80Δ* cells reiterates the patterns observed in *NDT80* cells (Figure 6E). Notably, accumulated JM levels in *msh5Δ ndt80Δ* cells are very low, no higher than the steady-state levels detected in *msh5Δ NDT80* cells. This observation suggests that the moderate steady-state JM levels detected in *msh5Δ NDT80* cells represent a small but very persistent population of molecules. Alternatively, the absence of Msh5 may permit JMs to be resolved via an Ndt80-independent mechanism, thereby preventing their accumulation in the *ndt80Δ* background.

Taken together, these data indicate that *sgs1-ΔC795* suppresses the crossover defect of *msh5Δ* cells by removing an impediment to the formation of crossover-specific precursors, dHJs. The most obvious interpretation is that Msh5 and Sgs1 are antagonistic with respect to dHJ formation.

DISCUSSION

The Extraordinary Meiotic Recombination Phenotype of *sgs1-ΔC795* Mutants

The observed patterns of crossing-over imply that DSBs that would normally form single crossovers in wild-type cells are more likely to result in closely spaced double crossovers in *sgs1-ΔC795* cells. The simplest interpretation of our data is that Sgs1 prevents closely spaced crossovers by preventing formation of JMs involving more than two chromatids.

Sgs1 Prevents Formation of Ternary and Quaternary JMs

The novel three and four duplex JMs identified in this study form at ~3-fold higher levels in *sgs1-ΔC795* cells. Ternary JMs are readily explained by a mechanism in which both DSB ends stably engage and prime DNA synthesis from different templates (Figure 7). This mechanism also dictates that at least one of the resulting D-loops migrates away from the DSB site to displace the extended 3′ end. The resulting end(s) can then anneal to connect the two D-loops and ultimately form a three duplex JM connected by two dHJs. Quaternary JMs require that one of the DSB ends sequentially invade two different templates before annealing occurs. Importantly, the DSB end must retain a plectonemic association with both template chromosomes. The final structure contains all four chromatids, interconnected by three dHJs (Figure 4A). The fact that ternary and quaternary JMs are detected in wild-type cells indicates that strand-exchange at both DSB ends and interaction with multiple templates are not peculiar to the *sgs1-ΔC795* situation and reflects the normal mechanism of meiotic recombination (see below).

Sgs1 Negatively Regulates Formation of Intersister dHJs

The >2-fold increase in IS-dHJs we detect by molecular assays correlates with increased recombination between sister chromatids in *sgs1* mutants (A.B.H. Chaix and R.H. Borts, personal communication). This phenotype cannot be due to a loss of interhomolog bias because interhomolog events remain high in *sgs1-ΔC795* tetrads. Instead, we suggest that while one DSB end interacts with the homolog, the other end frequently engages the sister chromatid, and that *sgs1-ΔC795* does not alter the overall frequency of intersister interactions but does alter their outcome. Specifically, we propose that Sgs1 normally disassembles intersister strand-exchange intermediates so that stable IS-dHJs and intersister crossovers form only rarely. We further propose that events that would normally give rise to simple interhomolog noncrossovers in wild-type cells may result in aberrant interhomolog noncrossovers with an associated sister-chromatid exchange in *sgs1-ΔC795* cells (Figure 7E).

A Multitemplate Mechanism Will Improve the Efficiency of Homologous Recombination

In canonical models of DSB repair, only one DSB end undergoes strand invasion and extension by polymerase, and the other end subsequently anneals to the product of this reaction (Paques and Haber, 1999). We propose a significant revision of these models, specifically that either or both DSB ends may undergo multiple rounds of invasion and extension from multiple templates. What could be the biological significance of allowing both DSB ends to

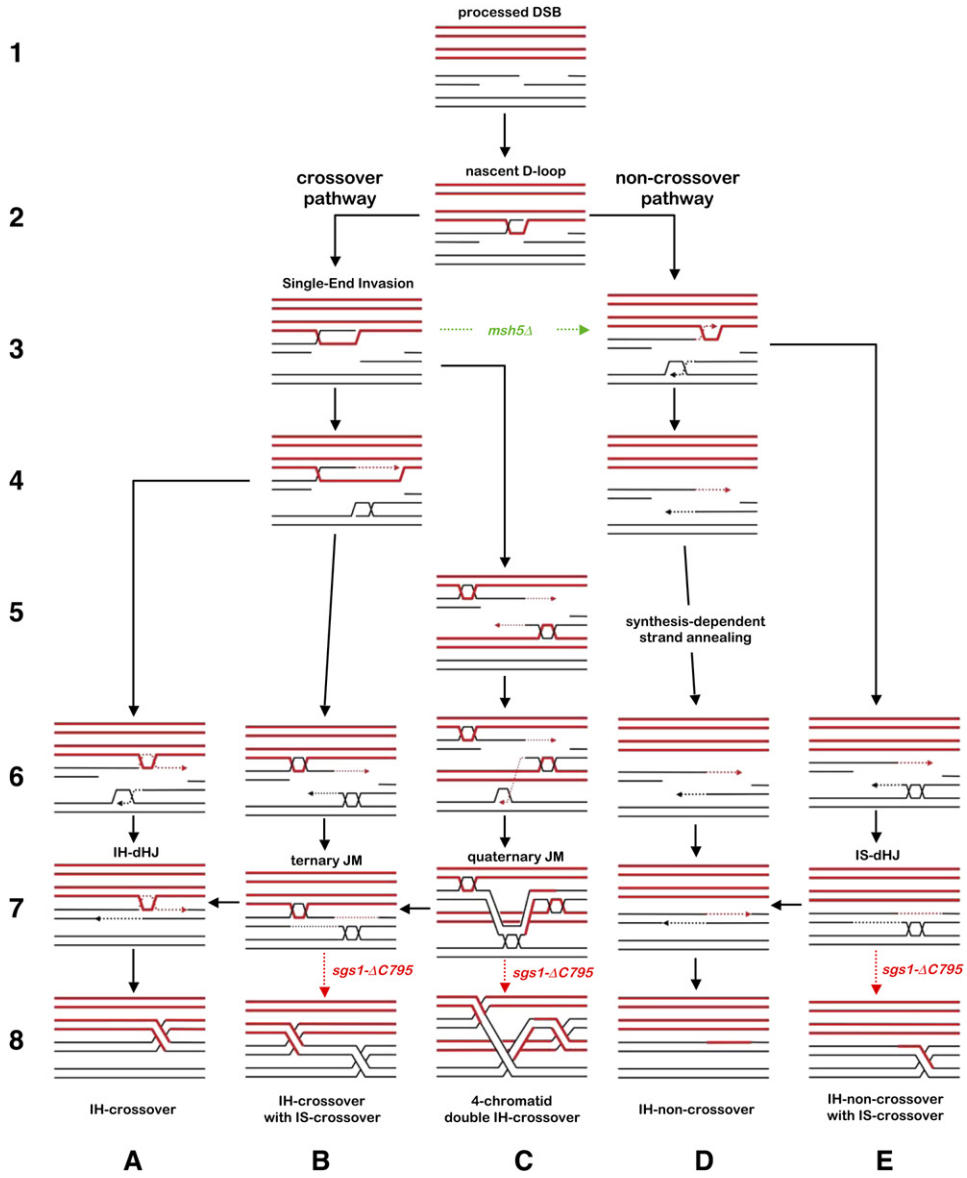

Figure 7. Model of Sgs1 (BLM) Function during Meiosis

Homologs are shown in red and black, respectively; dashed lines indicate nascent DNA. Solid black arrows indicate pathways in wild-type cells. Dashed arrows indicate pathways in mutants. The crossover or noncrossover decision follows pairing and strand invasion by one DSB end to form a nascent D-loop (steps 1 and 2; Borner et al., 2004; Hunter and Kleckner, 2001). Along the crossover pathway, ZMM proteins convert the nascent JM into a SEI, which is then stabilized by Msh4-Msh5 and Mlh1-Mlh3 antagonizing Sgs1 (steps 3B, 4B, and 6–8A; also see Jessop et al., 2006). Along the noncrossover pathway, the initial D-loop is not stabilized by ZMMs and ultimately disassembles even in the absence of Sgs1 (steps 3–8D). When homologs have successfully paired and synapsed, the sister chromatid (or any second homologous template) may be invaded by the second DSB end, e.g., steps 3D and 4B. Following extension by DNA synthesis, this end undergoes one of two annealing reactions with the first DSB end. At a crossover-designated site, the second DSB end anneals with the SEI to form a canonical dHJ, which is then resolved into a crossover (steps 6–8A). At a noncrossover site, the two DSB ends anneal to seal the break (steps 6–8D). Along both pathways, the helicase activity of Sgs1 (±Top3 strand-passage activity) ensures that the second DSB end completely dissociates from the template duplex. This could occur early, by disrupting the D-loop intermediate, or late, by dissolving dHJs formed by the second DSB end. In *sgs1-ΔC795* cells, the second DSB end does not efficiently disengage from its template and forms a stable dHJ independently of the first DSB end, e.g., steps 5C, 6B, and 6E. Along the crossover pathway, this will lead to formation of a ternary JM, which may be resolved into adjacent interhomolog (IH) and intersister (IS) crossovers (steps 6–8B). Successive invasion of two templates by a DSB end will give a quaternary JM, whose resolution can produce a four-chromatid double crossover (steps 5–8C). Along the noncrossover pathway, stable dHJ formation by the second DSB end will produce an IH-noncrossover associated with an IS exchange (steps 6–8E). D-loop migration and "end-first" strand displacement are proposed to be a common step that precedes strand annealing to form mature JMs. This mechanism readily accommodates the formation of multichromatid JMs. Strand displacement was previously proposed to explain the occurrence of DSB-distal JMs that lack intervening heteroduplex DNA (Allers and Lichten, 2001b).

interact with different template chromosomes? Most obvious is that the ability to extend either or both DSB ends will improve the efficiency of late steps of recombination. For example, during SDSA, extension of both DSB ends will produce longer and thus more efficiently annealed homologous single strands following end dissociation. Similarly, the transition from SEIs to dHJs will be more efficient if both DSB ends can be extended prior to annealing. In addition, the flexibility afforded by being able to extend either DSB end can overcome topological or steric hindrances in the template chromosome(s) that may limit extension from one or both ends. Finally, reiterative rounds of invasion coupled to weakly processive DNA synthesis may improve the fidelity of DSB repair by limiting nonproductive interactions, e.g., with dispersed repeats and templates with limited homology.

Meiotic Procrossover Factors Antagonize the Anticrossover Activity of Sgs1

Suppression of the meiotic defects of *msh5Δ* and *mlh3Δ* mutants by *sgs1-ΔC795* reveals a robust anticrossover activity for Sgs1 in the absence of procrossover factors. Jessop et al. (2006) recently described a similar suppressive effect of *sgs1* mutation on the crossover defects of *msh4Δ, mer3Δ, zip1Δ*, and *zip2Δ* mutants. In that study, although the degree of suppression varied from mutant to mutant, *msh4Δ* was efficiently suppressed, as we have observed for *msh5Δ*. Together, these observations suggest that a key function of meiotic procrossover factors, particularly the Msh4-Msh5 and Mlh1-Mlh3 complexes, is to antagonize the anticrossover activity of Sgs1. It should be noted, however, that *msh5Δ sgs1-ΔC795* cells still progress through meiosis more slowly than *MSH5* cells, indicating that Msh4-Msh5 has meiotic functions beyond simply antagonizing Sgs1. Moreover, the observations that (1) the *sgs1-ΔC795* single mutant does not show a simple hypercrossover phenotype and (2) the crossover defects of *mer3Δ* and *zip2Δ* are relatively poorly suppressed by *sgs1-ΔC795* (Jessop et al., 2006) indicate that, in addition to antagonizing Sgs1, some or all ZMMs are necessary for normal implementation of meiotic crossovers even in the absence of Sgs1.

Sgs1 Prevents dHJ Formation in the Absence of Msh5

In the case of *msh5Δ* cells, our in vivo data directly confirm the proposal that Sgs1 (and, by extension, BLM) can prevent dHJ formation. Sgs1 could decrease detected dHJs by disrupting SEIs and/or by dissolving dHJs as soon as they form. Our data do not clearly discriminate between these two possibilities.

Differential Activity of Procrossover Factors and Sgs1 at the Two DSB Ends Promotes the Orderly Formation of a Single dHJ at Designated Crossover Sites

The closely spaced crossovers, multichromatid JMs, and increased IS-dHJs in *sgs1-ΔC795* cells are reconciled by our proposal that both DSB ends can engage different template chromosomes to more efficiently effect late steps of recombination (see above). How then can we also reconcile the interaction between procrossover activities, such as Msh4-Msh5 and Mlh1-Mlh3, and Sgs1? We propose that procrossover factors act at designated crossover sites to stabilize interhomolog strand invasion by one DSB end, in part by antagonizing Sgs1. The antirecombination activity of Sgs1 then acts locally to disassemble JMs involving the second DSB end and, perhaps, to disrupt crossover precursors formed at other nearby DSB sites. Our model also explains why immunostaining foci of Sgs1 and BLM colocalize with procrossover factors along yeast and mouse meiotic chromosomes (Moens et al., 2002; Rockmill et al., 2003). How Sgs1 is recruited to recombination sites is unclear, but Sgs1 and BLM interact with a number of repair factors including Mlh1, Rad51, and the single-strand binding protein RPA (Hickson, 2003). Ultimately, this local coordination of pro- and anticrossover activities effects a type of local positive interference by ensuring that only one dHJ forms at sites that have been designated a crossover fate. Consequently, the risk of forming closely spaced crossovers is minimized.

Closely spaced crossovers are predicted to be nonproductive for meiosis because there will be little if any intervening cohesion, i.e., the homologs will no longer be connected (see Maguire, 1980; Nilsson and Sall, 1995; van Veen and Hawley, 2003). In addition, Rockmill et al. (2006) demonstrated that aneuploidy due to precocious separation of sister chromatids is associated with centromere-proximal crossing-over and proposed that such exchanges disrupt centromere cohesion. Undetected crossovers (between sisters or homologs) derived from multichromatid JMs could contribute to this effect. More generally, we conclude that the primary function of BLM and Sgs1 during homologous recombination, in both meiotic and somatic cells, is to help minimize the risk of potentially deleterious crossovers while also maximizing repair efficiency and fidelity by allowing strand invasion and extension at both DSB ends.

EXPERIMENTAL PROCEDURES

Yeast Strains and Genetic Techniques

Strains are derived from isolate SK1 (Table S7). Strains used to analyze crossing-over in Figure 1 are as described in de Los Santos et al. (2003), except that the *can1* mutation was omitted and the *arg4-bgl* allele was introduced using two-step gene replacement. The *HIS4LEU2* locus has been described (Hunter and Kleckner, 2001; Martini et al., 2006). The *sgs1-ΔC795* allele was constructed via oligonucleotide-mediated truncation using the *hphMX4* cassette (Goldstein and McCusker, 1999). *msh5Δ* and *mlh3Δ* mutations were made by replacing gene coding sequences with the *kanMX4* cassette (Wach et al., 1994). The *ndt80Δ* mutation was kindly provided by Thorsten Allers and Michael Lichten (Allers and Lichten, 2001a).

Tetrad Analysis

Haploid strains were mated briefly (≥3 hr) on YPD plates and sporulated on plates containing 1% potassium acetate and 0.02% raffinose at 30°C for 48–72 hr. Asci were digested with zymolyase and dissected

onto YPD plates. Only tetrads producing four viable spores were used in map distance calculations using the formula of Perkins (1949). Although the fraction of tetrads with four viable spores is reduced from 89% in wild-type to 51% in *sgs1-ΔC795*, calculated map distances do not appear to be biased since crossover frequencies in spores from tetrads both with full viability and with less than four viable spores are not different (data not shown). Standard errors were calculated using Stahl Lab Online Tools (http://groik.com/stahl/). Heterogeneity in segregation patterns was tested using log-likelihood G-tests as described (Hoffmann et al., 2003).

Meiotic Time Courses and DNA Physical Assays

Meiotic time courses were essentially as described by Goyon and Lichten (1993). DNA physical assays were performed as described previously (Schwacha and Kleckner, 1995; Hunter and Kleckner, 2001; Martini et al., 2006). Ratios of Mom and Dad strands for the "pull-apart" experiment were estimated using ImageQuant Version 5.0 (Molecular Dynamics). Integrated pixel intensities of areas corresponding to the signals of interest were compared after subtracting the background baseline. A correction was made for the fact that nonspecific nicking is incurred during crosslink reversal, which leads to biased reduction of signals for the longer Mom-length strands.

Electron Microscopy

DNA was isolated from gels and prepared for EM by the formamide spreading technique (Cromie et al., 2006; Davis et al., 1971). JMs were measured as detailed by Cromie et al. (2006). Contour lengths were converted to base pairs using a conversion factor of 0.34 nm per bp.

Supplemental Data

Supplemental Data includes six figures, seven tables, Supplemental Experimental Procedures, and Supplemental References and can be found with this article online at http://www.cell.com/cgi/content/full/130/2/259/DC1/.

ACKNOWLEDGMENTS

We thank Rhona Borts for communicating unpublished data, Michael Lichten for stimulating discussions and suggestions, and Wolf Heyer, Amitabh Nimonkar, and members of the Hunter lab for critical reading of the manuscript. N.H. is a Damon Runyon Scholar supported by the Damon Runyon Cancer Research Foundation (DRS-#40-04). This work was also supported by NIH NIGMS grants GM074223 to N.H. and GM031693 to G.R.S.

Received: January 10, 2007
Revised: April 18, 2007
Accepted: May 15, 2007
Published: July 26, 2007

REFERENCES

Allers, T., and Lichten, M. (2001a). Differential timing and control of noncrossover and crossover recombination during meiosis. Cell *106*, 47–57.

Allers, T., and Lichten, M. (2001b). Intermediates of yeast meiotic recombination contain heteroduplex DNA. Mol. Cell *8*, 225–231.

Argueso, J.L., Wanat, J., Gemici, Z., and Alani, E. (2004). Competing crossover pathways act during meiosis in *Saccharomyces cerevisiae*. Genetics *168*, 1805–1816.

Bachrati, C.Z., and Hickson, I.D. (2003). RecQ helicases: suppressors of tumorigenesis and premature aging. Biochem. J. *374*, 577–606.

Bachrati, C.Z., and Hickson, I.D. (2006). Analysis of the DNA unwinding activity of RecQ family helicases. Methods Enzymol. *409*, 86–100.

Bell, L., and Byers, B. (1983a). Separation of branched from linear DNA by two-dimensional gel electrophoresis. Anal. Biochem. *130*, 527–535.

Bell, L.R., and Byers, B. (1983b). Homologous association of chromosomal DNA during yeast meiosis. Cold Spring Harb. Symp. Quant. Biol. *47*, 829–840.

Bennett, R.J., Keck, J.L., and Wang, J.C. (1999). Binding specificity determines polarity of DNA unwinding by the Sgs1 protein of *S. cerevisiae*. J. Mol. Biol. *289*, 235–248.

Bishop, D.K., and Zickler, D. (2004). Early decision; meiotic crossover interference prior to stable strand exchange and synapsis. Cell *117*, 9–15.

Borner, G.V., Kleckner, N., and Hunter, N. (2004). Crossover/noncrossover differentiation, synaptonemal complex formation, and regulatory surveillance at the leptotene/zygotene transition of meiosis. Cell *117*, 29–45.

Chaganti, R.S., Schonberg, S., and German, J. (1974). A manyfold increase in sister chromatid exchanges in Bloom's syndrome lymphocytes. Proc. Natl. Acad. Sci. USA *71*, 4508–4512.

Cromie, G.A., Hyppa, R.W., Taylor, A.F., Zakharyevich, K., Hunter, N., and Smith, G.R. (2006). Single Holliday Junctions are intermediates of meiotic recombination. Cell *127*, 1167–1178.

Davis, R.W., Simon, R.W., and Davidson, N. (1971). Electron microscope heteroduplex methods for mapping regions of base sequence homology in nucleic acids. Methods Enzymol. *21*, 413–428.

de Los Santos, T., Hunter, N., Lee, C., Larkin, B., Loidl, J., and Hollingsworth, N.M. (2003). The Mus81/Mms4 endonuclease acts independently of double-Holliday junction resolution to promote a distinct subset of crossovers during meiosis in budding yeast. Genetics *164*, 81–94.

Ellis, N.A., Groden, J., Ye, T.Z., Straughen, J., Lennon, D.J., Ciocci, S., Proytcheva, M., and German, J. (1995). The Bloom's syndrome gene product is homologous to RecQ helicases. Cell *83*, 655–666.

Gangloff, S., McDonald, J.P., Bendixen, C., Arthur, L., and Rothstein, R. (1994). The yeast type I topoisomerase Top3 interacts with Sgs1, a DNA helicase homolog: a potential eukaryotic reverse gyrase. Mol. Cell. Biol. *14*, 8391–8398.

Goldstein, A.L., and McCusker, J.H. (1999). Three new dominant drug resistance cassettes for gene disruption in *Saccharomyces cerevisiae*. Yeast *15*, 1541–1553.

Goyon, C., and Lichten, M. (1993). Timing of molecular events in meiosis in *Saccharomyces cerevisiae*: stable heteroduplex DNA is formed late in meiotic prophase. Mol. Cell. Biol. *13*, 373–382.

Grushcow, J.M., Holzen, T.M., Park, K.J., Weinert, T., Lichten, M., and Bishop, D.K. (1999). *Saccharomyces cerevisiae* checkpoint genes *MEC1, RAD17* and *RAD24* are required for normal meiotic recombination partner choice. Genetics *153*, 607–620.

Hickson, I.D. (2003). RecQ helicases: caretakers of the genome. Nat. Rev. Cancer *3*, 169–178.

Hoffmann, E.R., and Borts, R.H. (2004). Meiotic recombination intermediates and mismatch repair proteins. Cytogenet. Genome Res. *107*, 232–248.

Hoffmann, E.R., Shcherbakova, P.V., Kunkel, T.A., and Borts, R.H. (2003). *MLH1* mutations differentially affect meiotic functions in *Saccharomyces cerevisiae*. Genetics *163*, 515–526.

Hollingsworth, N.M., Ponte, L., and Halsey, C. (1995). MSH5, a novel MutS homolog, facilitates meiotic reciprocal recombination between homologs in Saccharomyces cerevisiae but not mismatch repair. Genes Dev. *9*, 1728–1739.

Hunter, N. (2006). Meiotic recombination. In Molecular Genetics of Homologous Recombination, A. Aguilera and R. Rothstein, eds. (Heidelberg: Springer-Verlag), pp. 381–442.

Hunter, N., and Kleckner, N. (2001). The single-end invasion: an asymmetric intermediate at the double-strand break to double-Holliday junction transition of meiotic recombination. Cell *106*, 59–70.

Ira, G., Malkova, A., Liberi, G., Foiani, M., and Haber, J.E. (2003). Srs2 and Sgs1-Top3 suppress crossovers during double-strand break repair in yeast. Cell *115*, 401–411.

Jessop, L., Rockmill, B., Roeder, G.S., and Lichten, M. (2006). Meiotic chromosome synapsis-promoting proteins antagonize the anti-Crossover activity of Sgs1. PLoS Genet *2*, e155. 10.1371/journal.pgen.0020155.

Johnson, R.D., and Jasin, M. (2001). Double-strand-break-induced homologous recombination in mammalian cells. Biochem. Soc. Trans. *29*, 196–201.

Kadyk, L.C., and Hartwell, L.H. (1992). Sister chromatids are preferred over homologs as substrates for recombinational repair in *Saccharomyces cerevisiae*. Genetics *132*, 387–402.

Karow, J.K., Constantinou, A., Li, J.L., West, S.C., and Hickson, I.D. (2000). The Bloom's syndrome gene product promotes branch migration of Holliday junctions. Proc. Natl. Acad. Sci. USA *97*, 6504–6508.

Keeney, S. (2001). Mechanism and control of meiotic recombination initiation. Curr. Top. Dev. Biol. *52*, 1–53.

Kolas, N.K., and Cohen, P.E. (2004). Novel and diverse functions of the DNA mismatch repair family in mammalian meiosis and recombination. Cytogenet. Genome Res. *107*, 216–231.

Langland, G., Kordich, J., Creaney, J., Goss, K.H., Lillard-Wetherell, K., Bebenek, K., Kunkel, T.A., and Groden, J. (2001). The Bloom's syndrome protein (BLM) interacts with MLH1 but is not required for DNA mismatch repair. J. Biol. Chem. *276*, 30031–30035.

Lipkin, S.M., Moens, P.B., Wang, V., Lenzi, M., Shanmugarajah, D., Gilgeous, A., Thomas, J., Cheng, J., Touchman, J.W., Green, E.D., et al. (2002). Meiotic arrest and aneuploidy in MLH3-deficient mice. Nat. Genet. *31*, 385–390.

Maguire, M.P. (1980). Adaptive advantage for chiasma interference: a novel suggestion. Heredity *45*, 127–131.

Martini, E., Diaz, R.L., Hunter, N., and Keeney, S. (2006). Crossover homeostasis in yeast meiosis. Cell *126*, 285–295.

Moens, P.B., Kolas, N.K., Tarsounas, M., Marcon, E., Cohen, P.E., and Spyropoulos, B. (2002). The time course and chromosomal localization of recombination-related proteins at meiosis in the mouse are compatible with models that can resolve the early DNA-DNA interactions without reciprocal recombination. J. Cell Sci. *115*, 1611–1622.

Mullen, J.R., Kaliraman, V., and Brill, S.J. (2000). Bipartite structure of the SGS1 DNA helicase in *Saccharomyces cerevisiae*. Genetics *154*, 1101–1114.

Mullen, J.R., Nallaseth, F.S., Lan, Y.Q., Slagle, C.E., and Brill, S.J. (2005). Yeast Rmi1/Nce4 controls genome stability as a subunit of the Sgs1-Top3 complex. Mol. Cell. Biol. *25*, 4476–4487.

Muller, H.J. (1916). The mechanism of crossing over. Am. Nat. *50*, 193–221.

Nassif, N., Penney, J., Pal, S., Engels, W.R., and Gloor, G.B. (1994). Efficient copying of nonhomologous sequences from ectopic sites via P-element-induced gap repair. Mol. Cell. Biol. *14*, 1613–1625.

Nilsson, N.O., and Sall, T. (1995). A model of chiasma reduction of closely formed crossovers. J. Theor. Biol. *173*, 93–98.

Opresko, P.L., Cheng, W.H., and Bohr, V.A. (2004). Junction of RecQ helicase biochemistry and human disease. J. Biol. Chem. *279*, 18099–18102.

Paques, F., and Haber, J.E. (1999). Multiple pathways of recombination induced by double-strand breaks in *Saccharomyces cerevisiae*. Microbiol. Mol. Biol. Rev. *63*, 349–404.

Pedrazzi, G., Perrera, C., Blaser, H., Kuster, P., Marra, G., Davies, S.L., Ryu, G.H., Freire, R., Hickson, I.D., Jiricny, J., and Stagljar, I. (2001). Direct association of Bloom's syndrome gene product with the human mismatch repair protein MLH1. Nucleic Acids Res. *29*, 4378–4386.

Perkins, D. (1949). Biochemical mutants in the smut fungus *Ustilago maydis*. Genetics *34*, 607–626.

Petronczki, M., Siomos, M.F., and Nasmyth, K. (2003). Un menage a quatre: the molecular biology of chromosome segregation in meiosis. Cell *112*, 423–440.

Plank, J.L., Wu, J., and Hsieh, T.S. (2006). Topoisomerase IIIalpha and Bloom's helicase can resolve a mobile double Holliday junction substrate through convergent branch migration. Proc. Natl. Acad. Sci. USA *103*, 11118–11123.

Pochart, P., Woltering, D., and Hollingsworth, N.M. (1997). Conserved properties between functionally distinct MutS homologs in yeast. J. Biol. Chem. *272*, 30345–30349.

Richardson, C., Stark, J.M., Ommundsen, M., and Jasin, M. (2004). Rad51 overexpression promotes alternative double-strand break repair pathways and genome instability. Oncogene *23*, 546–553.

Rockmill, B., Fung, J.C., Branda, S.S., and Roeder, G.S. (2003). The Sgs1 helicase regulates chromosome synapsis and meiotic crossing over. Curr. Biol. *13*, 1954–1962.

Rockmill, B.M., Voelkel-Meiman, K., and Roeder, G.S. (2006). Centromere-proximal crossovers are associated with precocious separation of sister chromatids during meiosis in *Saccharomyces cerevisiae*. Genetics *174*, 1745–1754.

Schwacha, A., and Kleckner, N. (1994). Identification of joint molecules that form frequently between homologs but rarely between sister chromatids during yeast meiosis. Cell *76*, 51–63.

Schwacha, A., and Kleckner, N. (1995). Identification of double Holliday junctions as intermediates in meiotic recombination. Cell *83*, 783–791.

Schwacha, A., and Kleckner, N. (1997). Interhomolog bias during meiotic recombination: meiotic functions promote a highly differentiated interhomolog-only pathway. Cell *90*, 1123–1135.

Shinohara, A., and Shinohara, M. (2004). Roles of RecA homologues Rad51 and Dmc1 during meiotic recombination. Cytogenet. Genome Res. *107*, 201–207.

van Brabant, A.J., Ye, T., Sanz, M., German, I.J., Ellis, N.A., and Holloman, W.K. (2000). Binding and melting of D-loops by the Bloom syndrome helicase. Biochemistry *39*, 14617–14625.

van Veen, J.E., and Hawley, R.S. (2003). Meiosis: When even two is a crowd. Curr. Biol. *13*, R831–R833.

Wach, A., Brachat, A., Pohlmann, R., and Philippsen, P. (1994). New heterologous modules for classical or PCR-based gene disruptions in *Saccharomyces cerevisiae*. Yeast *10*, 1793–1808.

Wang, T.F., and Kung, W.M. (2002). Supercomplex formation between Mlh1-Mlh3 and Sgs1-Top3 heterocomplexes in meiotic yeast cells. Biochem. Biophys. Res. Commun. *296*, 949–953.

Wang, T.F., Kleckner, N., and Hunter, N. (1999). Functional specificity of MutL homologs in yeast: evidence for three Mlh1-based heterocomplexes with distinct roles during meiosis in recombination and mismatch correction. Proc. Natl. Acad. Sci. USA *96*, 13914–13919.

Watt, P.M., Hickson, I.D., Borts, R.H., and Louis, E.J. (1996). *SGS1*, a homologue of the Bloom's and Werner's syndrome genes, is required for maintenance of genome stability in *Saccharomyces cerevisiae*. Genetics *144*, 935–945.

Woods, L.M., Hodges, C.A., Baart, E., Baker, S.M., Liskay, M., and Hunt, P.A. (1999). Chromosomal influence on meiotic spindle assembly: abnormal meiosis I in female Mlh1 mutant mice. J. Cell Biol. *145*, 1395–1406.

Wu, L., Bachrati, C.Z., Ou, J., Xu, C., Yin, J., Chang, M., Wang, W., Li, L., Brown, G.W., and Hickson, I.D. (2006). BLAP75/RMI1 promotes the BLM-dependent dissolution of homologous recombination intermediates. Proc. Natl. Acad. Sci. USA *103*, 4068–4073.

Wu, L., and Hickson, I.D. (2003). The Bloom's syndrome helicase suppresses crossing over during homologous recombination. Nature *426*, 870–874.